

©2010 IEEE. Personal use of this material is permitted. However, permission to reprint/republish this material for advertising or promotional purposes or for creating new collective works for resale or redistribution to servers or lists, or to reuse any copyrighted component of this work in other works must be obtained from the IEEE.

# Vehicle Combustion Quality Monitoring: A scene visibility-level based non-invasive approach\*

Masood Mehmood Khan

Mechanical Engineering Department, Curtin University  
Kent Street, Bentley Campus, Perth, Australia, 6845

**Abstract**— Pollutants interfere with light, restrict its reflection and so impair visibility. Scene visibility level is therefore used as a measure of air quality and pollution. Treating emission efflux as “some additional noise causing visibility impairment,” this work examines if the extracted visibility index from a thermal infrared (TIR) image can help in qualitative assessment of combustion efficiency. The thin-film regime like two dimensional TIR images of unleaded-petroleum run vehicles’ exhaust-plumes were first accommodated for time and space related compositional effects. The estimated ratios of visibility indices obtained from two sequential TIR images of the same exhaust plume were compared with their respective electrochemically sensed levels of oxides of nitrogen and combustibles. Initial results suggest that visibility indices extracted from TIR images of emission efflux would help in distinguishing low from high levels of emissions. TIR images can therefore assist in qualitative assessment of engine combustion efficiency.

**Keywords**—non-invasive combustion analysis, vehicle exhaust plume image analysis, thermal infrared imaging application

## I. INTRODUCTION

Both primary and secondary pollutants behave like particles in the atmospheric air. Primary pollutants result from a combustion process whereas secondary pollutants are formed when the primary pollutants interact and trigger some chemical reactions [1,2,3]. Pollutants scatter back radiation into space, become the nucleus of raindrops, cause irritation to human lungs and throats and reduce visibility [2,3].

The Oxford English dictionary defines visibility as “the condition, state, or fact of being visible” [4]. In everyday conversation, visibility relates to the appearance of a vista or prospect. Visibility impairment therefore relates to a noticeable change in the appearance of a prospect, scene or vista. Under normal atmospheric conditions, presence of ambient levels of fine particulates (sulfate compounds, nitrate compounds, carbon elements, soil compounds and compounds of other organic matters) does not impair human visibility. Pollutants, when added to a view interfere with visibility and obstruct clear observation of scenes [5,6]. Visibility can be measured using one of the several available methods reported in [6,7]. Measurements of atmospheric visibility have been employed for determining air quality, pollution and presence of particulate matters and gaseous species [5,6,8].

Visible-spectrum imaging has been successfully employed for monitoring air quality changes through examination of visibility parameters [5]. However, visibility measurement within the visible spectrum can be illumination variant and less sensitive to the scene variations. The visible spectrum images therefore cannot provide highly accurate visibility indices under lighting and brightness conditions. Thermal infrared (TIR) imaging allows illumination-invariant measurement of visual and thermal features of ambient environment [9].

The spectroscopic and thermographic techniques can provide reliable estimates of the mass flow rates and the concentrations of species within the combustion exhaust efflux [10,13]. Theoretically, identifying molecular species and estimating their concentration within a plume sample are attainable with either TIR imaging or spectroscopy. However, observed spectral features cannot provide readily interpretable information about the molecular concentrations of the species within the exhaust plume [10,13].

The infrared emission from the molecules within a gaseous medium can be directly influenced by the temperature and concentration. Thus the two most important pieces of information, absolute radiant intensity and relative spectral shape are easily lost, particularly in optically thin gaseous regimes. Though several methods and techniques have been developed to estimate the spatial and temporal variations in temperature, the intensities of measured spectral features cannot be directly related with the molecular concentrations of species within the exhaust plume [10]. Hence, interpreting combustion efficiencies from thermographic information is a tedious task that involves stoichiometric estimations and complex thermodynamic calculations. Nonetheless, TIR imaging has demonstrated the potential for possible application in non-invasive engine combustion analysis.

This work explores the possibility of using TIR imaging for qualitative assessment of unleaded petroleum run light passenger vehicle emissions under normal atmospheric conditions. The exhaust emissions are treated as added noise to a TIR scene. The atmospheric visibility in a TIR scene is then used for examining the influence of exhaust plume on the visibility. The measured indices of visibility are compared with the levels of oxides of nitrogen and combustibles for qualitative assessment of unleaded petroleum run engines’ combustion efficiencies. The proposed approach is expected to lessen our reliance on the prevailing

\* Published in the proceedings of the 11<sup>th</sup> IEEE International Conference on Control, Automation, Robotics and Vision (ICARCV 2010), 7-10 Dec. 2010, Singapore, ISBN 978-1-4244-7813-2.

methods of combustion efficiency monitoring and therefore will help combustion regulatory bodies in distinguishing acceptable from unacceptable levels of vehicle emissions.

The following sections respectively present some relevant theoretical information, employed experimental design, a proposed visibility measurement algorithm, results and analysis. The work is finally concluded at the end.

## II. THEORETICAL BACKGROUND

Behaving like gas particles, pollutants interact with light through absorption and scattering. Consequently, the interaction between particles and light causes: light scattering by particles, light scattering by gases, light absorption by particles and light absorption by gases. Particles cause scattering of light coming from the objects and thus affect their visibility [6].

In volumetric terms, a great majority (more than 90%) of internal combustion engine emissions constitutes CO<sub>2</sub>, H<sub>2</sub>O and N<sub>2</sub> [10,11]. In a typical emission exhaust sample, the remaining constituents are: oxides of nitrogen (NO<sub>x</sub>), carbon monoxide (CO), unburned hydrocarbons, partially oxidized hydrocarbons, sulfur dioxide (SO<sub>2</sub>), particulates and smoke [10,14]. The CO<sub>2</sub> emission results when a hydrocarbon fuel is combusted near or above stoichiometric conditions. The produced SO<sub>x</sub> typically include SO, S<sub>2</sub>O, S<sub>n</sub>O, SO<sub>2</sub>, SO<sub>3</sub> and SO<sub>4</sub>. However, only SO<sub>2</sub> and SO<sub>3</sub> are of greater importance in combustion studies [14]. In a combustion efflux, oxides of nitrogen generally include nitrogen monoxide and nitrogen dioxide but may also include nitrous oxide and nitrogen tetroxide [10,14]. In most high-temperature combustion processes, the exhaust plume would usually contain oxides of nitrogen that rapidly combine with the atmospheric O<sub>2</sub> and forms NO<sub>2</sub>, a reddish brown gas [14]. NO<sub>x</sub> contributes to formation of smog and acid rain. In cases of incomplete fuel combustion, two types of combustibles; CO and volatile organic compounds (VOCs), are produced [10,14]. CO is a flammable, colorless non-corrosive gas. VOCs are low-molecular weight aliphatic and aromatic hydrocarbons. Typical VOCs include acetone, benzene, chloroform, formaldehyde, methanol and toluene and so they can cause photochemical smog when released in the atmosphere [14]. Particulates are also produced as a result of combustion process. The produced particulates look dirty in their various forms and can contribute to smog [14]. Particulate matters, oxides of nitrogen and SO<sub>x</sub> also contribute to the visibility impairment [15].

TIR imaging measures the radiant electromagnetic energy (expressed in radiance Watts/steradian-cm<sup>2</sup>) within the infrared region of electromagnetic spectrum. Basically, an IR camera would collect heat energy measurements and transform these measurements into a voltage signal. In other words, the digital counts are transformed into radiance values, which in turn, are converted into temperature measurements using the emissivity estimates of the target object [16].

The ability of a particular compound, that is part of a combustion efflux, to emit or absorb radiation can be exploited for its characterization and identification [9,14]. The fact that no chemical species can emit or absorb radiation beyond a particular band of electromagnetic spectrum has been helpful in TIR detection of species within combustion products [9,14, 17,18].

## III. EXHAUST EFFLUX FLOW AND DIFFUSION

For the purpose of combustion quality analysis, an exhaust efflux could be treated as a mixture of fully and partially burned gas particles [2,3]. The unstable eddies in the air would cause such a plume of combustion exhaust to diverge and disappear in the atmosphere. Transport of any concentration of pollutants within the exhaust plume would typically involve: transport of matter; transport of momenta in the flowing medium; and transport of energy. These three transport processes are governed by a set of well defined physical principles. These processes have been described using well-defined mathematical models [2,3,12].

The kinetic theory of gases and the Fick's law of heat diffusion suggest that the exhaust efflux travels from the regions of high concentration to the regions of low concentration. The relevant physical laws provide a framework for analyzing the exhaust efflux and pollutant diffusion. The exhaust efflux and pollutant diffusion modeling approach employed in this work was validated using the methods and techniques proposed in [12]. The major assumption behind the employed efflux and pollutant diffusion approach was that any turbulent diffusion would result in the pollutant dispersion. Therefore, for an adequate approximation, general diffusion equations were used to estimate the effect of turbulence on the efflux diffusion.

The concentration of a pollutant at a certain position in a gaseous medium would, in time, distribute over the entire expansion of the gas [2,3]. If the sample volume is carefully picked, the molecular diffusion can be considered a minor factor in the distribution of pollutants [1,2,3]. This can be understood by considering the effect of diffusion on the concentration  $C(x, y, z) = C(r)$  of a diffusing substance defined as:

$$C = \frac{\Delta M}{\Delta V} \quad (1)$$

M is the mass and V is the sample volume of the diffusing substance in equation 1. If a sample is selected such that  $\Delta V$  can be assumed to be appropriately proportional to  $a^3$  ( $a$  being the mean free path between the diffusing particles) then it becomes easy to accommodate for a change in  $C$  with the time [1,2]. Also,  $C(r)$  is assumed to be a continuous and differentiable function. With a proper sampling approach, the  $C$  can be significantly reduced. Therefore,  $C$  gets very small and the change in mass volume can be assumed as negligible. In this work the thermal images of the exhaust effluxes were taken at the exhaust-origin. Each image was

then divide into two equal pixel-size images and instead of estimating the magnitude of  $C$ , the rate of change in  $C$  within the two segments of the same image was used to estimate the visibility indices that prevailed in the two individual segments of a TIR image.

Another factor, the flow of gases also influences the pollutant concentration and their distribution [2,3]. Two measures were taken to control this factor. Firstly, an instantaneous image of exhaust efflux was taken at the exhaust outlet leaving very little time for the gaseous mixture to flow away or mix with the atmosphere [12]. Secondly, instead of looking at the overall concentration of pollutants in the efflux sample, the change in the pollutant concentration within the two segments of an instantaneous thermal image was taken into account for combustion quality assessment. Thus the influence of air flow was minimized.

#### IV. EXPERIMENTAL DESIGN

Five unleaded petroleum-run vehicle engines were tested at a predetermined engine speed of 2000 revolutions per minute. A long-wave (8.0-14.0  $\mu\text{m}$ ) infrared camera was used for thermography in this work. The camera was set half a meter away, normal to the exhaust efflux stream, to ensure a consistent and pre-determined Field of View. The thermal images of exhaust emissions were taken right at the exhaust pipe outlet to minimize the effects of rapid mixing and dispersion of pollutants in the atmosphere [2,3]. Also, efforts were made to avoid a turbulent atmosphere while capturing the exhaust plume images.

In order to avoid any complex background, a low-emissivity background (Styrofoam,  $\epsilon = 0.50-0.55$ ) was used during the thermal imaging. An electrochemical-sensors supported emission/combustion analyzer was used for emission analysis and measuring the combustion efficiencies of the tested vehicle engines. Figure 1 exhibits the infrared imaging and combustion analysis arrangements and an acquired thermal image of emission efflux.

Figure 2 exhibits the visible-spectrum and linearly enhanced TIR images of a Honda Civic's engine exhaust plume.

#### V. SCENE VISIBILITY-LEVEL MEASUREMENT

The levels of brightness in the TIR images, measured through the pixel grey-levels, was helpful in determining the visibility indices of images [6,8,19]. An 8-bit ( $d=8$ ) TIR image like the ones acquired for this would work result in 0-255 [ $(d)^2 = 256$ ], grey-levels such that 0 represented a dark black pixel and 255 represented a bright white pixel [19].

The TIR image pixel grey-levels have been characterized into two distinct information pieces: reflectance and illumination [20]. Reflectance corresponds to the amount of light reflected by a surface (of a view) and illumination corresponds to the amount of light incident on that surface. The fast spatial variations in a TIR image of a scene usually represent the amount of light being reflected whereas its illumination is represented by the slow spatial variations. This distinctive nature of spatial variations can be exploited through application of Homomorphic filtering [20]. The Homomorphic filtering technique helps in separating these spatial variations. Thus the prevailing visibility levels can be computed through the varying nature of spatial variations [9,21].

A Homomorphic filter can estimate the levels of spatial variations using two different parameters. Hence, the emission efflux could be separated from the background of a TIR image and the foreground intensity (exhaust plume) could be easily estimated. Establishing the relationship between the intensity (or visibility impairment) of an emission efflux and the measured levels of pollutant emissions provide useful qualitative information about the combustion efficiency.



Fig. 1. Top- thermal infrared imaging set up, Middle- combustion analysis set up, and Bottom -an exhaust plume thermal infrared image.

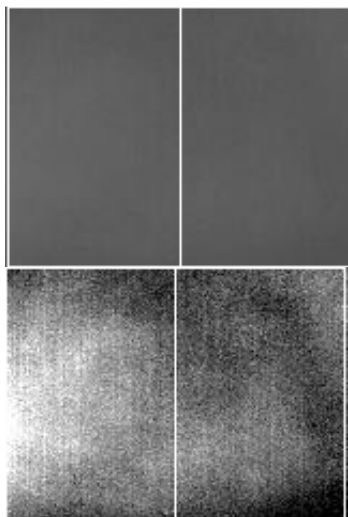


Fig. 2. Top: The original plume exhaust TIR image of a 2003 model Honda Civic. Bottom: The same image after linear-enhancement.

The Homomorphic filtering based algorithmic approach employed to estimate the visibility indices of the emission efflux TIR images is described in the following paragraphs.

1. Let the acquired TIR image  $g(r, c)$  be a product of **R**eflectance  $R(r, c)$  and **I**rradiance  $I(r, c)$ .
2. Assuming that the  $I(r, c)$  varies within the image, the variation in  $I(r, c)$  would cause some multiplicative noise that is usually such that the measured irradiance in a typical exhaust plume TIR image is  $I(r, c) \ll R(r, c)$ .

This would warrant a correction to transform the prevailing multiplicative noise into a measure of additive noise according as,

$$\log[g(r, c)] = \log[R(r, c)] + \log[I(r, c)];$$

3. The Fourier transform of the corrected TIR image  $\log [g(r, c)]$  is obtained;
4. The added noise,  $\log [I(r, c)]$  is eliminated by applying a high pass filter to the outcome of step 2;
5. The inverse Fourier transform of the outcome of step 3 is obtained as:

$$\tilde{g}_1(r, c) = \mathfrak{F}^{-1}[\mathfrak{H}(u, v)\mathfrak{F}\{\log[g(r, c)]\}];$$

6. Taking the exponential values of  $\tilde{g}_1(r, c)$  at every  $(r, c)$ , an averaged TIR is obtained by translating each exponential value (realized in step 5) into a corresponding grey-level between 0 and 255;
7. The grey-levels in the averaged TIR are then used to determine the intensity of foreground pixels (visibility impairment).

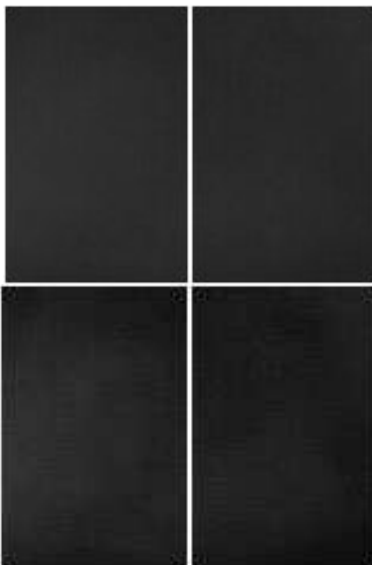


Fig 3. The original (top) and enhanced (bottom) TIR images of the same 2003 model Honda Civic after the algorithmic treatment.

## VI. RESULTS AND ANALYSIS

This work employed the time and space-averaged infrared images of emissions for determining the visibility ratio of the two sequential images. The employed approach resulted in an estimate of the visibility impairment within the prevailing atmospheric conditions.

Figure 3 (posted close to Figure 2 above) demonstrates how the proposed algorithm would change the visual contents of the exhaust plume TIR images. Figure 3 actually shows how the TIR images shown earlier in Figure 2 would change as a result of applying the filtering algorithm.

The ratio of the estimated Homomorphic filter indices ( $H$ ) for the two images of each vehicle plume, their measured levels of CO, CO<sub>2</sub>, NO, NO<sub>x</sub> and respective combustion efficiencies are reported in Table 1.

Figure 4 exhibits the relationship between the ratios of visibility indices and levels of measured NO in the five engines. The shown relationship corresponds to a correlation coefficient of 0.8012 and a linear regression line  $y=0.000433x+0.808$ .

The relationship between the ratios of visibility indices and levels of measured NO<sub>x</sub> in the five engines is shown in Figure 5. The shown relationship corresponded to a correlation coefficient of 0.7942 and a linear regression line  $y=0.00041x+0.808$ .

Similarly, Figure 6 exhibits the relationship between the ratio of visibility indices and the levels of measured combustibles

measured in the first four cars described in Table 1. The level of combustibles measured for the fifth car, a 2003 model Honda Civic, was not included in this analysis. The exhibited relationship corresponded to a correlation coefficient of -0.826 and a linear regression line  $y=-0.176x+0.862$ .

Though a small set of exhaust plume TIR images was available for this work and the tested car-engines had very similar combustion efficiencies (81.2% - 85.3%), these results seemed encouraging and promising. Based on the observed results, it would be safe to assume that a low combustion efficiency engine would be easy to distinguish from a high efficiency one using the proposed algorithmic approach.

A reliable estimate of the concentration of species within the exhaust plume could not be made through these observed results and relationships. Nonetheless, the observed visibility (and visibility impairment) estimates readily provide some interpretable information about the variations in the levels of unleaded petroleum-run combustion engines' operational efficiencies. In particular, having a strong correlation coefficient (greater than  $\pm 0.8$ ), the levels of NO (in ppm) and the amount of combustibles seem to be reflecting well on the observed visibility indices.

TABLE I  
COMBUSTION ANALYSIS RESULTS OF FIVE UNLEADED-PETROLEUM RUN CARS

Vehicle number and description	Visibility Ratio H <sub>1</sub> /H <sub>2</sub>	CO (ppm)	CO <sub>2</sub> (ppm)	NO (ppm)	NO <sub>x</sub> (ppm)	Combustibles (ppm)	Combustion efficiency (%)
1.Barina	0.833	67	12	0	84	0.5	81.2
2.Impreza	0.855	0	11.9	84	127	0.3	84.3
3.Corolla	0.853	0	11.9	121	10	0.1	85.3
4.Yaris	0.837	0	12	10	0	0.3	85.2
5.Civic	0.854	5	12	0	0	0.6	83.1

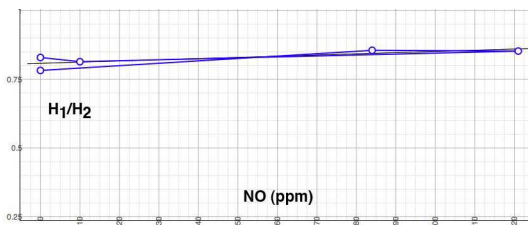


Fig 4. The ratios of visibility indices vs. the measured levels of NO.

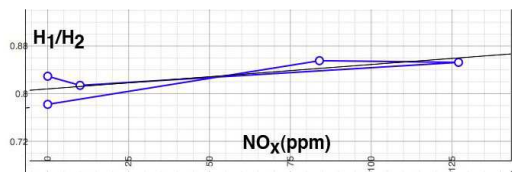


Fig 5. The visibility indices vs. the measured levels of NO<sub>x</sub>.

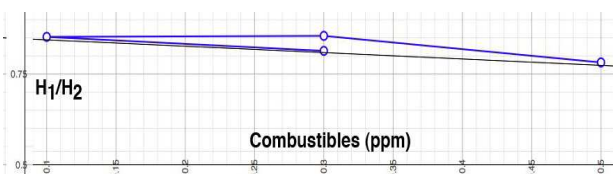


Fig 6. The estimated visibility indices vs. the measured levels of combustibles.

It must be noted that the near-linear nature of the relationships obvious in figures 4, 5 and 6 is based on analyses of a small set of passenger vehicles having similar (electrochemically measured) combustion efficiencies. These relationships might require further validation through an extension of this work. A larger database of exhaust efflux sample coming from various types of engine running on the same fuel might reveal the strength and weaknesses of these results. Also, including vehicles of varying engine conditions and different ages in a larger database of exhaust efflux sample and testing these vehicles in different driving and operating conditions might help.

## VII. CONCLUSION

This work treated unleaded petroleum run engine exhaust emissions as added noise to the prevailing atmospheric conditions within the TIR images and measured the influence of exhaust plume on the visibility for qualitatively determining the combustion efficiencies. A Homomorphic filtering based algorithmic approach was employed to compute the visibility indices in the plume exhaust TIR images. The observed relationships between the ratio of visibility in the two sequential exhaust plume images and the (separately) measured levels of combustibles and oxides of nitrogen seemed to be providing some useful and interpretable information about the combustion quality of tested engines. The reported initial results were encouraging and suggested that TIR imaging of exhaust plume might help combustion regulatory bodies to distinguish acceptable from unacceptable levels of vehicle emissions. These initial results require further validation though. A larger database of exhaust plume TIR images (taken from engines running under varying operational and atmospheric conditions) will be required to test and validate the proposed algorithmic approach and verify the observed results.

## VIII. ACKNOWLEDGEMENT

Yoannes Prima Singal Pranoto and Aditama Pratanu, two final year Mechatronic engineering students of the Department of Mechanical Engineering at Curtin University's Bentley campus, Perth, Western Australia, tested the reported engine combustion efficiencies and acquired the vehicle exhaust plume TIR images for this work.

## REFERENCES

- [1] A. Ramaswami, J.B. Milford and M.J. Small, *Integrated environmental modeling: Pollutant transport, fate and risk in the environment*. NJ: John Wiley and Sons, 2005.
- [2] E. Boeker and R. van Grondelle, *Environmental Physics*. NJ: John Wiley and Sons, 1995.
- [3] J.H. Seinfeld, *Atmospheric Chemistry and Physics*. NY: John Wiley and Sons, 1986.
- [4] *Oxford English Dictionary*, 9<sup>th</sup> edition. New York: Oxford University Press Inc., 2001.
- [5] W.C., Malm, J. Trijonis, J. Sisler, M. Pitchford, and R.L. Dennis, "Assessing the effect of SO<sub>2</sub> emission changes on visibility," *Atmospheric Environment*, vol.28, no.5, pp. 1023-1034, 1994.
- [6] N.P. Hyslop, "Impaired visibility: the air pollution people see," *Atmospheric Environment*, vol.43, pp. 182-195, 2009.
- [7] R.C. Henry, "A field study of visual perception of complex natural targets through atmospheric haze by naïve observers," *Atmospheric Environment*, vol.40, pp. 5251-5261, 2006.
- [8] J-J. Liaw, S-B. Lian, Y-F. Huang, and R-C. Chen, "Atmospheric visibility monitoring using digital image analysis techniques," in X. Jian and N. Petkov (Eds.), *Computer Analysis of Images and Patterns*, Lecture Notes in Computer Science 5702, pp. 1204-1211, Springer-Verlag, Berlin Heidelberg, 2009.
- [9] P.L. Hanst, "Infrared spectroscopy and infrared lasers in air pollution research and monitoring," *Applied Spectroscopy*, vol. 24, no. 2, pp. 161-174, 1970.
- [10] E.L. Keating, *Applied Combustion*. New York: Marcel Dekker Inc., 1993.
- [11] A.Faiz, C.S. Weaver, and M.P. Walsh, *Air Pollution from Motor Vehicles*. Washington, D.C.: The World Bank, 1996.
- [12] G.T. Scanady, *Turbulent diffusion in the environment*. Dordrecht, Netherlands: Kluwer Academic Publishing, 1973.
- [13] G.P. Jellison and D.P. Miller, "Determination of gas plume temperature from molecular emission spectra," *Optical Engineering*, vol. 45, no. 1, pp. 016201-1-8, 2006.
- [14] C.E., Baukal Jr., *Oxygen-enhanced combustion*, New York: CRC Press Inc., 1998.
- [15] T.E. Dzubay, R.K. Steven, C.W. Lewis, D.H. Hern, W.J. Courtney, J.W. Tesch, M.A. Mason, Visibility and aerosol composition in Houston, Texas. *Environmental Science and Technology* vol. 16, pp. 514-525, 1982.
- [16] P.W. Kurse, *Uncooled Thermal Imaging: Analysis, Systems and Applications*. Washington: SPIE Press, 2001.
- [17] J. Heland, and K. Scafer, "Determination of major combustion products in aircraft exhaust by FTIR emission spectroscopy," *Atmospheric Environment*, vol. 32, no.18, pp. 3067-72, 1998.
- [18] V. Tank, M. Hess, F. Schreier, and E. Lindermier, "Remote detection and quantification of hot molecular combustion products-experimental instrumentation and determination of optimal infrared spectral micro-windows," *Journal of Molecular Structure*, vol. 744-747, pp. 235-242, 2005.
- [19] L.B. Wolf, D.A. Socolinsky, C.K. Eveland, Face recognition in thermal infrared, in B. Bhanu and I. Pavlidis (Eds.), *Computer vision beyond visible spectrum*, London: Springer-Verlag, 2005.
- [20] T.G. Stockham Jr., "Image processing in the context of a visual model," *Proceedings of IEEE*, vol. 60, pp. 828-842, 1972.
- [21] R.C. Gonzalez, R.E. Woods, *Digital Image Processing*. New York: Prentice Hall, 2008.